Acta Neurochir (2012) 154:689–697
DOI 10.1007/s00701-012-1297-1

EXPERIMENTAL RESEARCH

iNOS-mediated secondary inflammatory response differs between rat strains following experimental brain contusion

Mattias Günther · Faiez Al Nimer · Caroline Gahm · Fredrik Piehl · Tiit Mathiesen

Received: 30 September 2011 / Accepted: 30 January 2012 / Published online: 24 February 2012

Abstract
Background Nitric oxide is a key mediator of post-traumatic inflammation in the brain. We examined the expressions of iNOS, nNOS, and eNOS in inbred DA and PVGa rat strains where DA is susceptible to autoimmune neuroinflammation and PVGa-resistant.
Methods Parietal contusions using a weight drop model were produced in five rats per genotype. After 24 h, the brains were removed and analyzed using a range of immunohistochemical methods.
Results PVGa presented significantly increased iNOS expression in infiltrating inflammatory cells in the perilesional area compared to DA ($p<0.05$). The amount of w3/13-positive infiltrating inflammatory cells did not differ between strains. eNOS and nNOS expression did not differ between strains. iNOS-positive cells coexpressed neuronal (NeuN), macrophage (ED-1), and leucocyte (w3/13) markers. MnSOD was significantly increased in PVGa ($p<0.05$). 3-Nitrotyrosine, a measure of peroxynitrite levels, and fluoro-jade stained neuronal degeneration, did not differ between strains.
Conclusions Two inbred rat strains with genetically determined differences in susceptibility to develop autoimmune disease displayed different levels of the inflammatory and anti-inflammatory mediators iNOS and MnSOD, indicating genetic regulation. Interestingly, the increased levels of iNOS did not lead to elevated expression of the neuronal cell-death marker fluoro-jade. The increased iNOS expression was correlated with increased expression of superoxide scavenger MnSOD. Excessive peroxynitrite formation was probably prevented by limitation of available superoxide. Subsequently, the higher expression of potentially deleterious iNOS in PVGa did not result in increased neuronal death.

Keywords Neurotrauma · Neuroinflammation · TBI · Nitric oxide synthase · Peroxynitrite · Manganese superoxide dismutase · Dark Agouti · Piebald Virol Glaxo

M. Günther (✉) · F. Al Nimer · C. Gahm · F. Piehl · T. Mathiesen
Department of Clinical Neuroscience, Section of Neurosurgery and Neuroimmunology, Karolinska Institutet,
SE-171 76 Stockholm, Sweden
e-mail: mattias.gunther@ki.se

Introduction

Traumatic brain injury (TBI) is a leading cause of death and disability among young adults in the industrialized world [1]. The injury results in a direct loss of viable brain tissue, worsened by secondary processes including inflammation, which may persist for months. The inflammation can be either detrimental or beneficial. The secondary processes are intricate, and despite extensive research, no substance has been found to have any positive effect on outcome, albeit there are many promising prospects [30, 20, 9, 34, 28]. Nevertheless, we and others have revealed that traumatic injuries in rodents, following identical experimental trauma settings as used in this study [15], have led to an inflammatory reaction with up-regulation of NOS isoenzymes and subsequent cerebral cell death [5, 26, 44, 2, 24, 45].

Nitric oxide

Nitric oxide (NO) is a key mediator in the inflammatory process [45]. Following TBI, NO reacts with superoxide to form peroxynitrite, a powerful toxic oxidant involved in secondary tissue injury. This includes DNA strand damage, attenuation of mitochondrial respiration, lipid peroxidation,

cell enzyme inhibition, cytoskeletal protein breakdown, and induction of apoptosis. NO has also been reported to be involved in potentially protective reactions [11, 32, 6]. Peroxynitrite is difficult to detect, which is why the more stabile parameter 3-Nitrothyrosine (3-NT), derived from NO_2 nitration of tyrosine residues in proteins, is often used as a stabile surrogate measure instead [6].

NO is formed by three NO synthases. Endothelial (eNOS) and neuronal (nNOS) isoforms are calcium-dependent and endogenously expressed in the brain, while the inducible (iNOS) isoform is expressed primarily in macrophages, microglia, infiltrating neutrophils, and to some extent in neurons. Independent of calcium, iNOS upregulates following trauma and has primarily detrimental effects. According to some studies, inhibition of iNOS has resulted in beneficial effects in lesion volume and sensorimotor outcome [45, 15, 18], while other studies demonstrate worse functional outcome and increased mortality following iNOS inhibition [39, 19, 24, 32]. These conflicting results may to some extent be related to genetic variability [43, 37, 41, 12, 23].

Genetic variation in neuroinflammation

The majority of TBI research has been performed on genetically heterogeneous rodents presenting quantitatively and qualitatively diverse inflammatory mechanisms. Inbred strains, however, may react reproducibly. Susceptibility to autoimmune inflammation in the CNS such as autoimmune encephalomyelitis (EAE) is strain dependent. The inbred rat Piebald Virol Glaxo (PVG) is resistant to EAE, while the strain Dark Agouti (DA) is highly susceptible [8, 47, 31, 46, 33]. This is relevant for TBI research as the inflammatory response is part of the pathogenesis. The PVG strain response to trauma is dominated by infiltrating polymorphonuclear granulocytes, while the DA strain expresses more T-cells, an enhanced glial activation and more C3 complement. DA strain rats acquire smaller lesions than PVG strain rats under similar experimental conditions [7, 3]. The three NOS enzymes are relevant mediators in trauma-induced inflammation, which is why we hypothesized that NOS expression might differ between DA and PVG strains following comparable TBI. In addition, we analyzed whether iNOS levels would correlate with peroxynitrite formation and neuronal death.

Materials and methods

Tissue preparation

The experiments were approved by the North Stockholm Animal Ethics Committee (Stockholms Norra djurförsöksetiska nämnd). All animals were housed at the Karolinska University Hospital (Stockholm, Sweden) in polystyrene cages containing aspen wood shavings and with free access to water and standard rodent chow with regulated 12-h light–dark cycles.

A total of ten male rats weighing approximately 230–300 g, at an age of 8–12 weeks, were anesthetized by intraperitoneal injection of 2.7 ml/kg of a mixture of Hyperoxynitriteorm (fluanisone, 10 mg/ml, fentanyl citrate, 0.315 mg/ml; Janssen, Oxford, UK), Dormicum (midazolam, 1 mg/ml, Roche) and sterile water. In addition, 0.2 ml of Marcain (bupivacaine, 5 mg/ml, AstraZeneca, Södertälje, Sweden) was injected subcutaneously in the sagittal midline of the skull before the skin incision was made. The rats were placed in a stereotactic frame and a 2-mm craniotomy was drilled 3 mm posterior and 2.3 mm lateral to the bregma. A standardized parietal contusion was made by letting a 24-g weight fall onto a rod with a flat end diameter of 1.8 mm from a height of 7 cm [10, 21]. The rod was allowed to compress the tissue at a maximum of 3 mm. All animals were killed with CO_2 at day 1 post-injury, brain tissue was removed and immediately snap-frozen in 2-methylbutane and stored at –70ºC. Then, 14-μm-thick coronal sections were cut using a Leica CM3000 cryostat and were mounted for subsequent staining. The sections extended from the frontal to the dorsal border of the parietal contusion, macroscopically verified to encompass contused brain matter. For the analyses, frontal, mid, and dorsal sections were averaged for each animal in order to better assess the complete lesion.

Immunohistochemistry

Primary and secondary antibodies for immunohistochemistry and immunofluorescence are shown in Table 1. Detection was performed by the ABC method (Vectastain Elite ABC peroxidase kit, Vector Labs, Burlingame, CA, USA) or immunofluorescence. All steps included washing three times 10 min each with phosphate buffer solution (PBS).

The ABC method: sections were rehydrated in PBS followed by fixation in 4% formaldehyde, incubation in 0.3% H_20_2, incubation for 1 h in bovine serum albumin (BSA) with 0.3% Triton X-100, NaAzid and avidin block solution, incubation overnight at 4 °C with the primary antibody diluted in 1% BSA, 0.3% Triton X-100, and NaAzid and biotin block solution. Sections incubated with nitrotyrosine antibody were prior to this heated for 3 min in antigen unmasking solution (Vector Labs H-3300) according to instructions. Sections were then incubated for 1 h with the appropriate biotinylated secondary antibody, and incubated with avidin-biotin complex for 1 h. Immunoreactivity was developed using DAB substrate for 3 min, which was stopped by rinsing in distilled water and Tris–HCl. Sections were then counterstained with hematoxylin III nach Gill (Merck, Darmstadt, Germany) for 15 s, dehydrated in

Table 1 Antibodies used

Antibody	Specificity	Species	Concentration	Lot	Source
iNOS	Inducible NOS	Rabbit	1:800	NA	Transduction Labs, Lexington, KY
eNOS	Endothelial NOS	Mouse	1:800	NA	Transduction Labs, Lexington, KY
nNOS	Neuronal NOS	Rabbit	1:800	NA	Transduction Labs, Lexington, KY
GFAP	Astrocytes	Mouse	1:500	LV1689941	Millipore, Temecula, CA
Nitrotyrosine	Nitrotyrosine	Rabbit	1:100	LV1634965	Millipore, Temecula, CA
ED-1	Macrophages/monocytes	Mouse	1:2000	010806	Serotec, Oxford, UK
W3/13	CD43 antigen on T-cells	Mouse	1:1000	NA	Sera-Lab, Sussex, UK
NeuN	Neuronal nucleus	Mouse	1:500	LV1427917	Millipore, Temecula, CA
MnSOD	MnSOD, clone MnS-1	Mouse	1:500	NJ1811049	Millipore, Temecula, CA
Cy3	Secondary, fluorescent	Do anti Rb	1:500	79935	Jackson Labs, West Grove, PA
Alexa 488	Secondary, fluorescent	Do anti Mo	1:500	436938	Molecular Probes, Eugene, OR
Biotinyl. ab	Secondary, ABC method	Go anti Rb	1:200	VO111	Vector Labs, Burlingame, CA
Biotinyl. ab	Secondary, ABC method	Ho anti Mo	1:200	S0809	Vector Labs, Burlingame, CA

alcohol, and mounted with Pertex (Histolab Products AB, Göteborg, Sweden).

Immunofluorescence: sections were rehydrated in PBS followed by fixation in 4% formaldehyde, incubation for 1 h in BSA with 0.3% Triton X-100 and NaAzid and incubated overnight at 4°C with the primary antibody diluted in 1% bovine serum albumin, 0.3% Triton X-100 and NaAzid. Following 1-h incubation with the secondary antibody, sections were mounted with Mowiol (Polysciences Inc. Eppelheim, Germany).

Fluoro-jade (Histochem Inc. Jefferson, AR. Lot 19) was used as a marker for neuronal degeneration [38]. It was diluted to a working solution of 0.00002% in 0.1% acetic acid, and sections were incubated for 30 min before being washed in distilled water and dried on a hot plate (approx. 50°C) and mounted with Pertex.

For iNOS, eNOS, ED-1, and W3/13, sections of rat spleen were used as positive controls, and for nNOS sections of rat cerebellum. To rule out any possibility of non-specific conjugate binding, 1% BSA was used instead of primary antibody in negative controls, resulting in absent staining. Sham-operated animals were used for baseline expression of NOS isoenzymes.

Quantification

For all quantification, the region of interest (ROI) was defined medially by the interhemispheric fissure, basally by the corpus callosum, and laterally by the lateral border of the right hemisphere (Fig. 1). The central necrotic part of the contusion was omitted from the ROI. All manual quantification was made in the ROI and presented as the total amount of positive cells in the region. All sections were blinded to the assessor.

Morphological identification and quantification of iNOS in DAB staining and immunofluorescence was performed according to our earlier studies [14, 15, 16, 17]. The amount of positive cells was determined manually in the ROI by the same assessor in 400× magnification using a Leica DMRB and a DM400B microscope equipped with a DFC320 camera. iNOS-positive cells were clearly visible, as presented in Figs. 5 and 7, contrasting from negative tissue and negative controls. For each animal, ten sections were analyzed.

For immunofluorescence, the filter used for Cy3 antibody was N2.1 (excitation filter 515–560 nm, suppression filter 590 nm) and for Alexa 488 antibody filter L4 (excitation filter 450–490 nm, suppression filter 515–560 nm). Double-staining immunofluorescence was used for the quantification of iNOS, W3/13, NeuN, and ED-1 ratio, for which two sections per animal were averaged. For W3/13, four sections were averaged.

Fluoro-jade was detected using a filter with excitation wavelength 495 nm and emission wavelength of 521 nm. Quantification was done by calculating the total number of positive cells in the ROI in 400× magnification. For each animal, four sections were averaged.

Quantification of 3-NT staining was performed in 400× magnification according to Hooper et al. [22], based on our

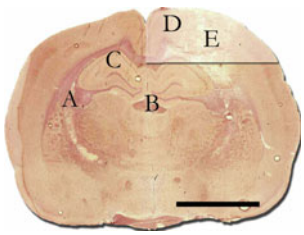

Fig. 1 Photo of coronal section of rat brain showing **a** lateral ventricle, **b** third ventricle, **c** hippocampus, **d** ROI=region of interest=elevated area in picture, and **e** contusion site (*scale bar* 3 mm)

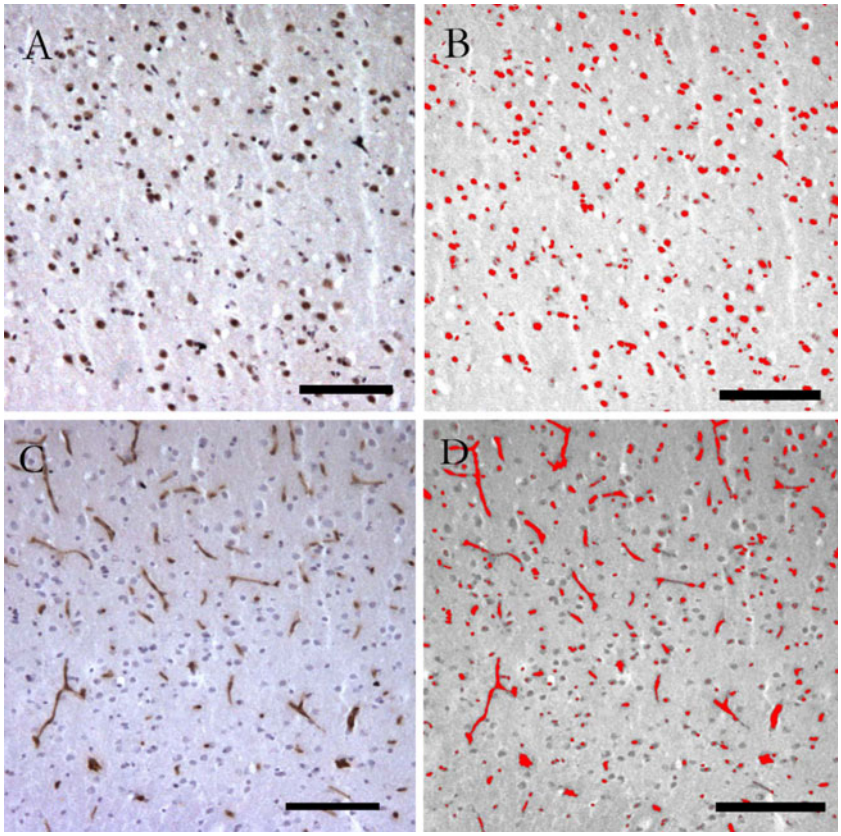

Fig. 2 Photomicrographs from the perilesional area showing **a** nNOS-positive cells, **b** marked area in *red* for quantification, **c** eNOS-positive endothelial cells, and **d** marked area in *red* for quantification. Counter-staining with hematoxylin (400×) (*scale bar* 50 μm)

earlier experiences of 3-NT staining [14, 18], with a slight modification to fit the ROI: 0=none, 1=1–20 positive loci of staining in ROI, 2=20–40 scattered discrete loci of staining or areas of weak staining, 3=extensive areas of strong staining. For each animal, six sections were analyzed.

For the quantification of eNOS and nNOS in DAB staining, two sections per animal and antibody were used. Six representative pictures per section were taken in the ROI in 100× magnification and converted into black and white using Adobe Photoshop CS and quantified in ImageJ (NIH, Bethesda, MA). An intensity threshold for which staining was regarded as positive was set above the negative control and applied equally for all quantified pictures using the automated threshold feature in ImageJ. Positive staining was for illustrative purposes marked in red and the number of pixels above the threshold (red area) was calculated and compared to the total number of pixels in each picture as shown in

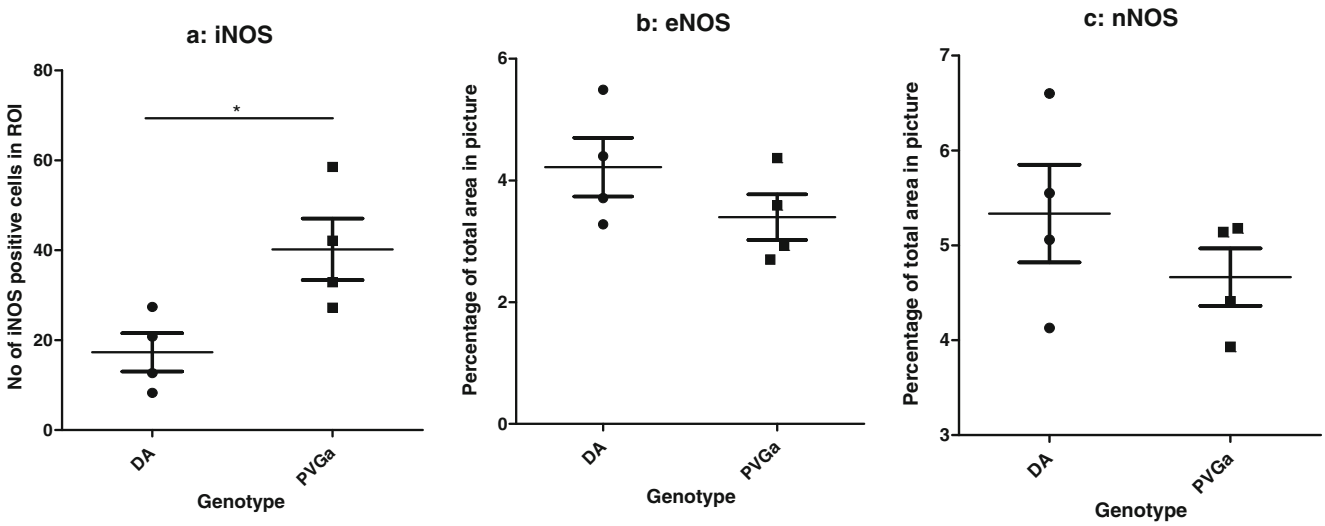

Fig. 3 **a**–**c** Immunohistochemical quantification at 24 h of **a** iNOS, **b** eNOS, and **c** nNOS. (*) iNOS expression is significantly raised in PVGa ($p<0.05$)

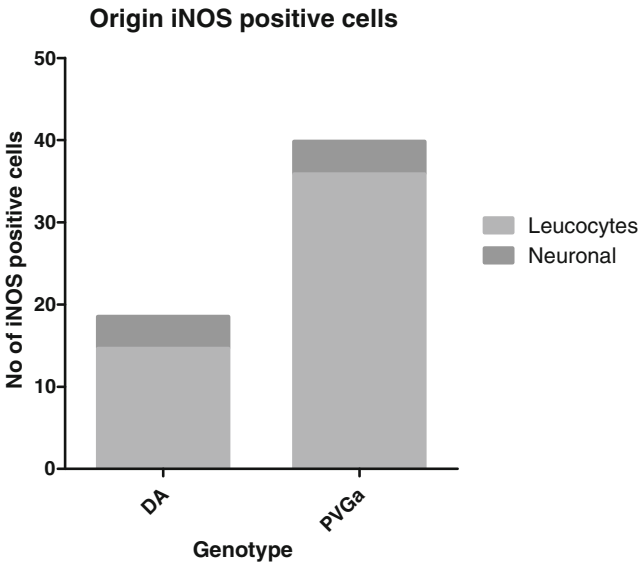

Fig. 4 Morphological differentiation of iNOS showing that the elevated expression of iNOS in PVGa was derived from leucocytes ($p<0.05$) while no significant difference in neurons could be detected

Fig. 2. The result was presented as a percentage of staining of the total area in each picture, reflecting the level of positive staining and the intensity of the staining.

The non-parametrical Kruskal–Wallis test was used for statistical analysis using GraphPad Prism (San Diego, CA, USA). A p value <0.05 was considered significant.

Results

The expression of iNOS was enhanced in the perilesional area in all rats subjected to contusion compared to controls, with no positive staining in the contralateral side. iNOS expression was significantly higher in PVGa rats compared to DA ($p<0.05$) (Fig. 3a). This difference was mainly attributed to a higher proportion of iNOS-positive inflammatory cells in PVGa than DA rats. The level of iNOS-positive neurons did not differ significantly between the strains (Figs. 4 and 5a–b).

The expression of eNOS and nNOS was diffusely enhanced in traumatized animals compared to controls, showing no difference between remote and perilesional areas. eNOS-positive cells were morphologically identified as endothelial cells and the majority of nNOS-positive cells as neurons (Fig. 2). No difference was detected between the genetic strains (Fig. 3b–c).

The level of inflammatory cells, detected by the w3/13 antibody, was enhanced in the perilesional area with very few positive cells found on the contralateral side. No difference was detected between the genetic strains (Fig. 6a).

Double-label immunofluorescence was performed with antibodies against iNOS and cellular markers for neurons (NeuN), macrophages (ED-1), and leucocytes (W3/13), respectively, in order to asses cellular origin of iNOS production (Fig. 7). No significant difference was detected between the genetic strains (Table 2).

MnSOD was expressed in the perilesional area in cells morphologically identified as neurons (Fig. 8). No positive cells were detected on the contralateral side. The number of MnSOD-expressing cells was significantly higher in PVGa rats compared to DA (Fig. 6b) ($p<0.05$).

3-NT expression was correlated with the primary location of iNOS-producing cells. 3-NT was mainly expressed in the perilesional area. No difference was detected between the genetic strains (Fig. 6c).

Fluoro-jade staining for neuronal degeneration presented a large number of positive cells with neuronal morphology in the perilesional area (Fig. 5c). No difference was detected between the strains (Fig. 6d).

Discussion

In this study, we conclude that iNOS expression following TBI differed between PVGa and DA rats at 24 h after TBI, predominantly in inflammatory cells. We regard this as a genotype-dependent difference, regardless of whether it is a difference of expression-kinetics or the total amount of iNOS. The variance was attributed to the proportion of iNOS-expressing cells rather than the total number of infiltrating inflammatory cells, which did not differ between strains. Unexpectedly, however, the iNOS differences did

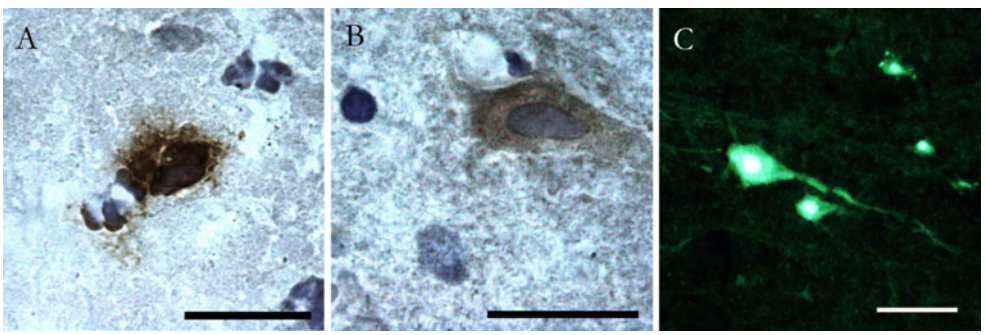

Fig. 5 Photomicrographs from the perilesional area showing **a** iNOS-positive leucocyte, **b** iNOS-positive neuron. Counterstaining with hematoxylin (1,000×). **c** Degenerating neurons positive for Fluoro Jade (400×). *Scale bar* 20 μm

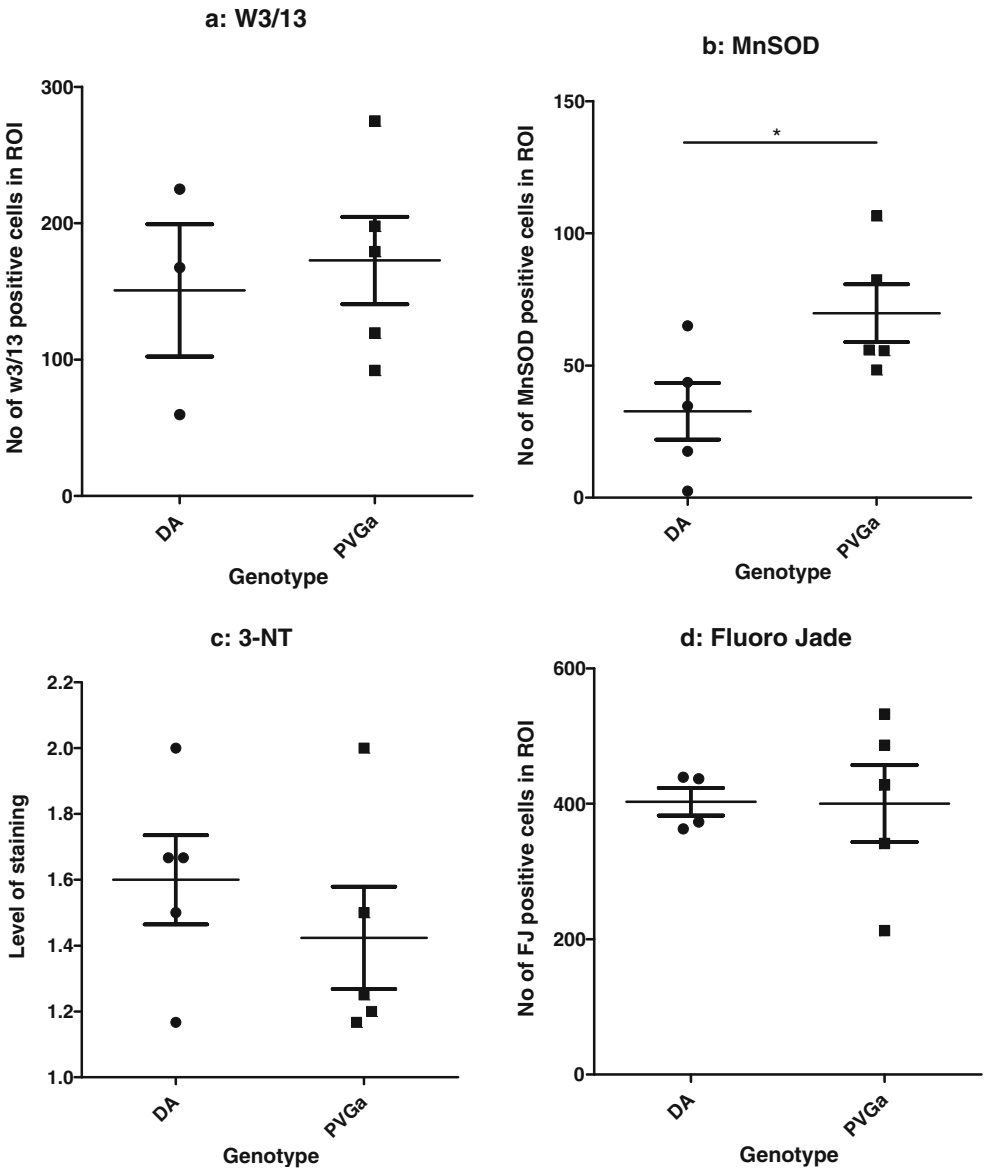

Fig. 6 **a**–**d** Immunohistochemical quantification at 24 h of **a** w3/13, **b** MnSOD, **c** 3-NT, **d** Fluoro Jade, in DA and PVGa rats, respectively. (*) MnSOD expression is significantly raised in PVGa ($p<0.05$)

not result in variable levels of 3-NT or fluoro-jade-positive dying neurons.

The study was designed to compare NO isoenzyme regulation between DA and PVGa rats following experimental TBI. According to our previous experience, NO isoenzymes are up-regulated in rodents exposed to TBI compared to sham-treated animals following an identical experimental trauma setting as used in this study [15]. This has further been confirmed for NOS isoenzymes and NO-derived products in diverse rodent strains and experimental trauma models [5, 26, 44, 2, 24, 45]. We therefore tried the hypothesis that variation of strains known to react diversely to EAE and

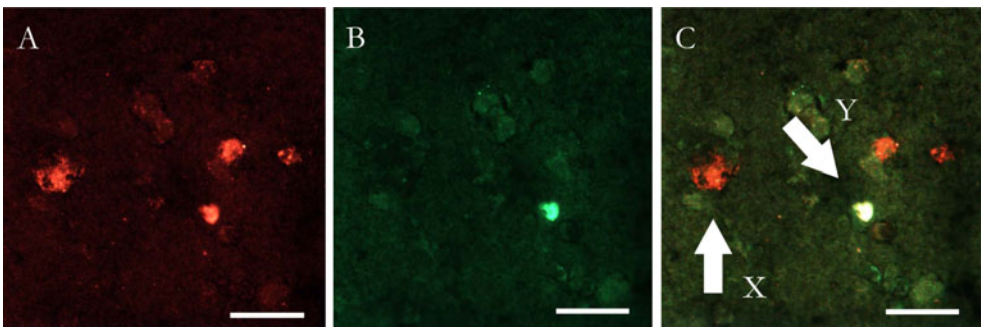

Fig. 7 Immunofluorescence photomicrographs of the perilesional area showing cells expressing **a** iNOS, **b** example of cellular marker: w3/13, and **c** merged pictures **a** and **b** showing (*arrow X*) a cell positive for iNOS only and (*arrow Y*) both iNOS and w3/13 (400×). *Scale bar* 20 μm

Table 2 Origin of iNOS-positive cells in double-staining immunofluorescence for iNOS and related cellular markers, presented for each antibody as a percentage of total iNOS-positive cells

Strain/antibody	NeuN	ED-1	W3/13
DA	<10%	50%	36%
PVGa	<10%	36%	34%

TBI [3, 7] would affect the NOS response, given a presumed elevation of NOS as described in earlier publications. For this reason, sham-treated animals were not used in the current setting since they would be irrelevant for the specific hypothesis and would weaken statistical power in comparison of the groups.

iNOS is a calcium-independent enzyme that is transcription-modulated by an array of inflammatory cytokines. It has a gene promoter with more than 20 binding sites for transcription factors, including NF-κB, STAT-1, IRF-1, and AP-1 [35]. It is therefore to a large extent regulated by inflammatory mechanisms. In contrast, eNOS and nNOS are calcium-dependent and catalytically regulated enzymes. The level of eNOS and nNOS expression did not differ between strains. They were diffusely up-regulated in the brain, while expression of iNOS was perilesional. These features probably reflect the different regulatory mechanisms.

NO reacts with superoxide, readily available in the perilesional area, to produce the toxic metabolite peroxynitrite [11, 32, 6]. Exposure to high concentrations of peroxynitrite may lead to rapid, necrotic-type cell death, as reviewed by Szabó et al. [42]. We assessed the level of peroxynitrite by using the stabile surrogate measure 3-NT. Unexpectedly, 3-NT expression did not differ between the genetic strains, nor did the neuronal degeneration. We conclude that the elevated expression of iNOS in PVGa rats did not result in a higher production of peroxynitrite or elevated neuronal death at 24 h after trauma.

NO production correlates to intracellular iNOS levels, but the formation of peroxynitrite also depends on the availability of superoxide. We therefore hypothesized that lower superoxide levels could limit peroxynitrite and 3-NT production in rats with higher iNOS levels. A number of endogenous protection mechanisms against superoxide have been described, including superoxide dismutase (SOD), peroxiredoxin V, selenium-containing amino acids and glutathione peroxidase, as reviewed by Arteel et al. [4] and Szabo et al. [42]. The SOD enzyme has three isoforms as reviewed by Fukai et al. [13]. Cytoplasmic Cu/ZnSOD (SOD1), mitochondrial MnSOD (SOD2), and extracellular Cu/ZnSOD (SOD3) all catalyze the dismutation of superoxide into O_2 and H_2O_2.

MnSOD is the first-line defense against superoxide generated in mitochondria; the major intracellular source of the superoxide radical. It upregulates in neurons and in activated microglia following increased superoxide formation [36]. Over-expression of MnSOD causes reduced lipid peroxidation, protein nitration, and neuronal death after experimental TBI [25] and MnSOD deficient mice perish at an early stage [29, 27].

MnSOD and iNOS were only detected in the perilesional areas, concurring with studies of ischemic brain injury [40]. Interestingly, we found that MnSOD was upregulated in PVGa rats compared to DA rats. It is probable that higher levels of MnSOD suppressed excessive formation of peroxynitrite, protecting the PVGa rat from unwarranted oxidative and nitrosative stress. The findings suggest a balance of the two potentially damaging and protective mechanisms. We cannot assess whether underlying genetic differences determined the higher iNOS and MnSOD expression in one strain, or whether a rapid adaptive regulation led to a secondary MnSOD synthesis in animals with higher levels of NO. An extended study with several earlier and later time-points could be expected to elucidate whether the strain difference reflects different kinetics of iNOS expression, or whether the total amount of iNOS differs. In addition, further time-points might show whether iNOS and MnSOD levels correlate at all time points, or whether MnSOD increases in a delayed fashion, as if secondarily induced. These analyses, together with exact quantification of the

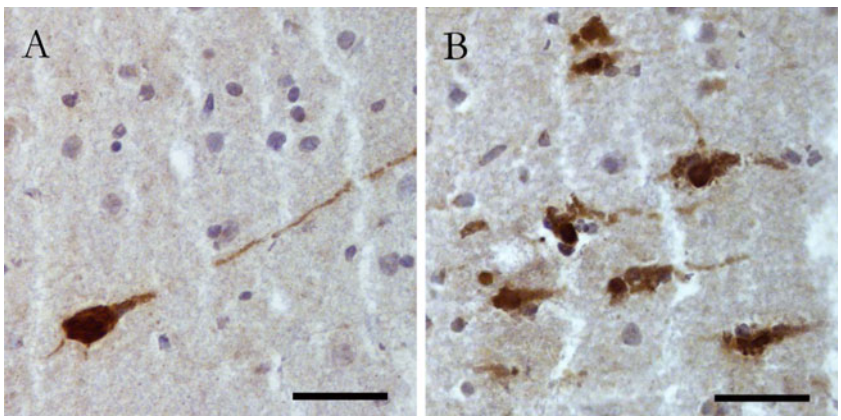

Fig. 8 Photomicrographs of the perilesional area showing **a** MnSOD-positive neurons with visible axon and **b** grouped MnSOD-positive neurons. Counterstaining with hematoxylin (400×). *Scale bar* 20 μm

reaction products, are necessary for a profound understanding, but include extensive analyses that are beyond the scope of this initial study.

Our results add to the growing knowledge that genetic factors alter the appearance of secondary inflammation following TBI. Our findings also highlight that a potentially relevant difference of one damaging substance may well lead to a secondary up-regulation of protective measures. The damaging and protective mechanisms are interrelated and it is necessary to explore how these balance each other under different circumstances and in different individuals. Indeed, a complex relationship between iNOS induction and neuronal death in the inflammatory environment is evolutionary probable. iNOS is mainly considered to be detrimental due to the induction of oxidative stress. However, iNOS knockout mice do worse than wild-type rodents in TBI experiments. In analogy with our findings, it may be speculated that an absence of iNOS may have been balanced by low levels of radical scavengers. The difference in oxidative defense may partly explain why the PVGa strain shows better resistance to neuroinflammatory induction protocols.

Conclusions

Following experimental TBI, iNOS expression was higher in PVGa rats than in DA rats. A genetically different pattern of post-traumatic inflammation was suggested. Interestingly, potentially protective MnSOD was also increased. Antioxidative protection mechanisms appeared to compensate for higher levels of iNOS, preventing additional peroxynitrite formation and neuronal death. We could not assess whether the differences reflect genetic programming or whether MnSOD levels represent a secondary increase induced by initial iNOS-catalyzed NO levels in PVGa rats.

Conflicts of interest None.

References

1. (1999) Consensus conference. Rehabilitation of persons with traumatic brain injury. NIH Consensus Development Panel on Rehabilitation of Persons With Traumatic Brain Injury. JAMA 282:974–983
2. Ahn ES, Robertson CL, Vereczki V, Hoffman GE, Fiskum G (2008) Normoxic ventilatory resuscitation following controlled cortical impact reduces peroxynitrite-mediated protein nitration in the hippocampus. J Neurosurg 108:124–131
3. Al Nimer F, Beyeen AD, Lindblom R, Strom M, Aeinehband S, Lidman O, Piehl F (2011) Both MHC and non-MHC genes regulate inflammation and T-cell response after traumatic brain injury. Brain Behav Immun 25:981–990
4. Arteel GE, Briviba K, Sies H (1999) Protection against peroxynitrite. FEBS Lett 445:226–230
5. Bayir H, Kagan VE, Borisenko GG, Tyurina YY, Janesko KL, Vagni VA, Billiar TR, Williams DL, Kochanek PM (2005) Enhanced oxidative stress in iNOS-deficient mice after traumatic brain injury: support for a neuroprotective role of iNOS. J Cereb Blood Flow Metab 25:673–684
6. Beckman JS, Beckman TW, Chen J, Marshall PA, Freeman BA (1990) Apparent hydroxyl radical production by peroxynitrite: implications for endothelial injury from nitric oxide and superoxide. Proc Natl Acad Sci USA 87:1620–1624
7. Bellander BM, Lidman O, Ohlsson M, Meijer B, Piehl F, Svensson M (2010) Genetic regulation of microglia activation, complement expression, and neurodegeneration in a rat model of traumatic brain injury. Exp Brain Res 205:103–114
8. Braden AW (1958) Strain differences in the incidence of polyspermia in rats after delayed mating. Fertil Steril 9:243–246
9. Eriksson PS, Perfilieva E, Bjork-Eriksson T, Alborn AM, Nordborg C, Peterson DA, Gage FH (1998) Neurogenesis in the adult human hippocampus. Nat Med 4:1313–1317
10. Feeney DM, Boyeson MG, Linn RT, Murray HM, Dail WG (1981) Responses to cortical injury: I. Methodology and local effects of contusions in the rat. Brain Res 211:67–77
11. Floyd RA (1999) Antioxidants, oxidative stress, and degenerative neurological disorders. Proc Soc Exp Biol Med 222:236–245
12. Friedman G, Froom P, Sazbon L, Grinblatt I, Shochina M, Tsenter J, Babaey S, Yehuda B, Groswasser Z (1999) Apolipoprotein E-epsilon4 genotype predicts a poor outcome in survivors of traumatic brain injury. Neurology 52:244–248
13. Fukai T, Ushio-Fukai M (2011) Superoxide dismutases: role in redox signaling, vascular function, and diseases. Antioxid Redox Signal 15:1583–1606
14. Gahm C, Danilov A, Holmin S, Wiklund PN, Brundin L, Mathiesen T (2005) Reduced neuronal injury after treatment with NG-nitro-L-arginine methyl ester (L-NAME) or 2-sulfo-phenyl-*N*-*tert*-butyl nitrone (S-PBN) following experimental brain contusion. Neurosurgery 57:1272–1281, discussion 1272–1281
15. Gahm C, Holmin S, Mathiesen T (2000) Temporal profiles and cellular sources of three nitric oxide synthase isoforms in the brain after experimental contusion. Neurosurgery 46:169–177
16. Gahm C, Holmin S, Mathiesen T (2002) Nitric oxide synthase expression after human brain contusion. Neurosurgery 50:1319–1326
17. Gahm C, Holmin S, Rudehill S, Mathiesen T (2005) Neuronal degeneration and iNOS expression in experimental brain contusion following treatment with colchicine, dexamethasone, tirilazad mesylate and nimodipine. Acta Neurochir (Wien) 147:1071–1084, discussion 1084
18. Gahm C, Holmin S, Wiklund PN, Brundin L, Mathiesen T (2006) Neuroprotection by selective inhibition of inducible nitric oxide synthase after experimental brain contusion. J Neurotrauma 23:1343–1354
19. Hlatky R, Lui H, Cherian L, Goodman JC, O'Brien WE, Contant CF, Robertson CS (2003) The role of endothelial nitric oxide synthase in the cerebral hemodynamics after controlled cortical impact injury in mice. J Neurotrauma 20:995–1006
20. Holmin S, Almqvist P, Lendahl U, Mathiesen T (1997) Adult nestin-expressing subependymal cells differentiate to astrocytes in response to brain injury. Eur J Neurosci 9:65–75
21. Holmin S, Mathiesen T (1996) Dexamethasone and colchicine reduce inflammation and delayed oedema following experimental brain contusion. Acta Neurochir (Wien) 138:418–424
22. Hooper DC, Scott GS, Zborek A, Mikheeva T, Kean RB, Koprowski H, Spitsin SV (2000) Uric acid, a peroxynitrite scavenger, inhibits CNS inflammation, blood-CNS barrier permeability changes, and

tissue damage in a mouse model of multiple sclerosis. FASEB J 14:691–698
23. Inman D, Guth L, Steward O (2002) Genetic influences on secondary degeneration and wound healing following spinal cord injury in various strains of mice. J Comp Neurol 451:225–235
24. Jafarian-Tehrani M, Louin G, Royo NC, Besson VC, Bohme GA, Plotkine M, Marchand-Verrecchia C (2005) 1400W, a potent selective inducible NOS inhibitor, improves histopathological outcome following traumatic brain injury in rats. Nitric Oxide 12:61–69
25. Keller JN, Kindy MS, Holtsberg FW, St Clair DK, Yen HC, Germeyer A, Steiner SM, Bruce-Keller AJ, Hutchins JB, Mattson MP (1998) Mitochondrial manganese superoxide dismutase prevents neural apoptosis and reduces ischemic brain injury: suppression of peroxynitrite production, lipid peroxidation, and mitochondrial dysfunction. J Neurosci 18:687–697
26. Khan M, Im YB, Shunmugavel A, Gilg AG, Dhindsa RK, Singh AK, Singh I (2009) Administration of S-nitrosoglutathione after traumatic brain injury protects the neurovascular unit and reduces secondary injury in a rat model of controlled cortical impact. J Neuroinflamm 6>
27. Lebovitz RM, Zhang H, Vogel H, Cartwright J Jr, Dionne L, Lu N, Huang S, Matzuk MM (1996) Neurodegeneration, myocardial injury, and perinatal death in mitochondrial superoxide dismutase-deficient mice. Proc Natl Acad Sci USA 93:9782–9787
28. Li L, Lu J, Tay SS, Moochhala SM, He BP (2007) The function of microglia, either neuroprotection or neurotoxicity, is determined by the equilibrium among factors released from activated microglia in vitro. Brain Res 1159:8–17
29. Li Y, Huang TT, Carlson EJ, Melov S, Ursell PC, Olson JL, Noble LJ, Yoshimura MP, Berger C, Chan PH, Wallace DC, Epstein CJ (1995) Dilated cardiomyopathy and neonatal lethality in mutant mice lacking manganese superoxide dismutase. Nat Genet 11:376–381
30. Lindholm D, Castren E, Kiefer R, Zafra F, Thoenen H (1992) Transforming growth factor-beta 1 in the rat brain: increase after injury and inhibition of astrocyte proliferation. J Cell Biol 117:395–400
31. Lorentzen JC, Andersson M, Issazadeh S, Dahlman I, Luthman H, Weissert R, Olsson T (1997) Genetic analysis of inflammation, cytokine mRNA expression and disease course of relapsing experimental autoimmune encephalomyelitis in DA rats. J Neuroimmunol 80:31–37
32. Lu J, Goh SJ, Tng PY, Deng YY, Ling EA, Moochhala S (2009) Systemic inflammatory response following acute traumatic brain injury. Front Biosci 14:3795–3813
33. Lundberg C, Lidman O, Holmdahl R, Olsson T, Piehl F (2001) Neurodegeneration and glial activation patterns after mechanical nerve injury are differentially regulated by non-MHC genes in congenic inbred rat strains. J Comp Neurol 431:75–87
34. Marklund N, Bakshi A, Castelbuono DJ, Conte V, McIntosh TK (2006) Evaluation of pharmacological treatment strategies in traumatic brain injury. Curr Pharm Des 12:1645–1680
35. Miljkovic D, Trajkovic V (2004) Inducible nitric oxide synthase activation by interleukin-17. Cytokine Growth Factor Rev 15:21–32
36. Noack H, Lindenau J, Rothe F, Asayama K, Wolf G (1998) Differential expression of superoxide dismutase isoforms in neuronal and glial compartments in the course of excitotoxically mediated neurodegeneration: relation to oxidative and nitrergic stress. Glia 23:285–297
37. Popovich PG, Wei P, Stokes BT (1997) Cellular inflammatory response after spinal cord injury in Sprague–Dawley and Lewis rats. J Comp Neurol 377:443–464
38. Schmued LC, Albertson C, Slikker W Jr (1997) Fluoro-Jade: a novel fluorochrome for the sensitive and reliable histochemical localization of neuronal degeneration. Brain Res 751:37–46
39. Sinz EH, Kochanek PM, Dixon CE, Clark RS, Carcillo JA, Schiding JK, Chen M, Wisniewski SR, Carlos TM, Williams D, DeKosky ST, Watkins SC, Marion DW, Billiar TR (1999) Inducible nitric oxide synthase is an endogenous neuroprotectant after traumatic brain injury in rats and mice. J Clin Invest 104:647–656
40. Ste-Marie L, Hazell AS, Bemeur C, Butterworth R, Montgomery J (2001) Immunohistochemical detection of inducible nitric oxide synthase, nitrotyrosine and manganese superoxide dismutase following hyperglycemic focal cerebral ischemia. Brain Res 918:10–19
41. Steward O, Schauwecker PE, Guth L, Zhang Z, Fujiki M, Inman D, Wrathall J, Kempermann G, Gage FH, Saatman KE, Raghupathi R, McIntosh T (1999) Genetic approaches to neurotrauma research: opportunities and potential pitfalls of murine models. Exp Neurol 157:19–42
42. Szabo C, Ischiropoulos H, Radi R (2007) Peroxynitrite: biochemistry, pathophysiology and development of therapeutics. Nat Rev Drug Discov 6:662–680
43. Teasdale GM, Nicoll JA, Murray G, Fiddes M (1997) Association of apolipoprotein E polymorphism with outcome after head injury. Lancet 350:1069–1071
44. Terpolilli NA, Zweckberger K, Trabold R, Schilling L, Schinzel R, Tegtmeier F, Plesnila N (2009) The novel nitric oxide synthase inhibitor 4-amino-tetrahydro-L-biopterine prevents brain edema formation and intracranial hypertension following traumatic brain injury in mice. J Neurotrauma 26:1963–1975
45. Wada K, Chatzipanteli K, Busto R, Dietrich WD (1998) Role of nitric oxide in traumatic brain injury in the rat. J Neurosurg 89:807–818
46. Weissert R, Wallstrom E, Storch MK, Stefferl A, Lorentzen J, Lassmann H, Linington C, Olsson T (1998) MHC haplotype-dependent regulation of MOG-induced EAE in rats. J Clin Invest 102:1265–1273
47. Wilson DB (1965) Quantitative Studies on the Behavior of Sensitized Lymphocytes in Vitro: I. Relationship of the Degree of Destruction of Homologous Target Cells to the Number of Lymphocytes and to the Time of Contact in Culture and Consideration of the Effects of Isoimmune Serum. J Exp Med 122:143–166